JOURNAL OF CATALYSIS 151, 50–59 (1995)

Textural Properties and Catalytic Activity of Hydrotalcites

Didier Tichit,* Mohammed Hassane Lhouty,* Alain Guida,* Bich Huong Chiche,* François Figueras,* Aline Auroux,† Davide Bartalini,‡ and Edoardo Garrone‡

*Laboratoire de Chimie Organique Physique et Cinétique Chimique Appliquées, U.A 418 C.N.R.S., E.N.S.C.M., 8 Rue École Normale, 34075 Montpellier Cedex, France; †Institut de Recherches sur la Catalyse, 2 Avenue Albert Einstein, 69626 Villeurbanne Cedex, France; and ‡Dipartimento di Chimica Inorganica, Chimica Fisica e Chimica dei Materiali, Università di Torino, Via P. Giuria 7, 10125 Turin, Italy

Received March 8, 1993; revised May 11, 1994

Double-layered hydroxides with hydrotalcite structure were synthesized with Mg/Al atomic ratios of 2.5 and 3 and with different contents of exchangeable Cl^- and CO_3^{2-} anions. The basicity of these solids depends on several structural parameters and on the activation temperature. Microcalorimetric measurements, IR spectroscopy using a probe molecule, and a catalytic test reaction were carried out to characterize the basic sites. The structural evolution of the hydrotalcite upon exchange of Cl^- for CO_3^{2-} and calcination temperature shows a transformation with simultaneous removal of CO_2 and water without phase segregation up to 673 K. The mixed oxide formed later could reversibly lead to the layered structure upon rehydration and carbonation. This process was studied by microcalorimetry and IR spectroscopy. The adsorption isotherm of CO_2 shows an increase of the uptake and consequently of the basicity with initial CO_3^{2-} content and calcination temperature up to 800 K. IR spectroscopy shows that the carbonation of the mixed oxide is essentially superficial and that the hydrotalcite structure may be restored upon H_2O addition and 373-K treatment. Two types of Lewis acid sites related to a linear coordination of CO_2 with Mg^{2+} and Al^{3+} cations are assigned. The appearance of a bicarbonate species implies that the basic sites are essentially OH groups. Moreover, a small number of strong basic sites, adsorbing CO_2 with 140 kJ/mol, probably correspond to O^{2-} centers. Hammett correlation in the condensation reaction of acetone and different substituted benzaldehydes shows analogies between hydrotalcite catalysis and the homogeneous basic reaction. The activities increase with CO_3^{2-} content, calcination temperature, and Mg/Al ratio of the hydrotalcites. The basic strength of hydrotalcites is comparable to that of piperidine in homogeneous catalysis. © 1995 Academic Press, Inc.

INTRODUCTION

Hydrotalcite-like compounds are double-layered hydroxides with general formula $(M^{2+}_{1-x}M^{3+}_x(OH)_2)^{x+}(A^{m-}_{x/m}) \cdot nH_2O$, where the divalent ion may be Mg^{2+}, Ca^{2+}, Zn^{2+}, or Ni^{2+}, the trivalent ion, Al^{3+}, Fe^{3+}, Cr^{3+}, ..., and the compensation anions, OH^-, Cl^-, NO_3^-, CO_3^{2-}, SO_4^{2-}, and x can take values between 0.25 and 0.33 (1, 2). It is an alternating layered structure with positively charged brucite-like layers $(M^{2+}_{1-x}M^{3+}_x(OH)_2)^{x+}$, where M^{2+} cations are substituted by M^{3+} cations, and interlayers containing the charge-balancing anions and water molecules. Many systems have been synthesized (3–7) with the purpose of obtaining anion exchangers (8, 9) or adsorbents. The adsorption of nitrogen, oxygen, carbon dioxide, and hydrogen on these solids has been investigated (10).

Ion exchange of the original anions by voluminous polyanions has also been achieved with the aim of obtaining pillared structures developing high surface areas and molecular sieving properties (11, 12).

The structural modifications occurring upon thermal treatment have been investigated by X-ray diffraction, thermal analysis, and specific surface area and pore volume measurements (13–16). Thermal treatments induce dehydration, dehydroxylation, and loss of the charge-compensating anions, resulting in mixed oxides with MgO-type structure. Hydrotalcites are consequently a class of precursors useful for the preparation of catalytically active oxides showing basic properties.

The activity and selectivity of these solids have been established for several reactions such as aldol condensation (17), olefin isomerization (18), alcohols from syngas (19), and nucleophilic halide exchange (20). Most of the studies were performed on Mg–Al mixed hydroxides. The system based on carbonates was found to be more active in several reactions (17). Synthetic Mg–Al hydrotalcites have been compared to other solids with moderate basic strength such as Cs–X and –Y zeolites, and Cs–sepiolites using reactants with different pK_a values (21, 22). These hydrotalcites are active in various condensation reactions of carbonyl compounds with activated methylenic compounds known as the Knoevenagel, Michael, Claisen-Schmidt reactions and aldolizations in organic chemistry depending on the nature of the compounds (23). They contain basic sites with pK_a values in the range 10.7–13.3 and a few sites with $pK_a = 16.5$. Such basicities stimulate their use as catalysts in industry as

0021-9517/95 $6.00

substitutes for liquid NaOH or KOH solutions to produce less polluting processes.

However, the influence of structural parameters and activation procedure on the basicity of hydrotalcites has not yet been fully explored. The present work is devoted to the influence of two structural parameters of Mg–Al hydrotalcites, namely, the CO_3^{2-} content and the Mg/Al ratio, and of the activation temperature on the basic properties. X-ray diffraction, FT-IR spectroscopy, thermogravimetric analysis, and volumetric and calorimetric measurements of the adsorption of CO_2 were used to analyze the structural modifications. The condensation of benzaldehyde and acetone, a reaction rather sensitive to catalyst basicity, was employed to study the change of basicity of these catalysts.

EXPERIMENTAL

Preparation of Hydrotalcites

Aqueous solutions containing 0.3 mol of $MgCl_2 \cdot 6H_2O$, 0.1 mol of $AlCl_3 \cdot 6H_2O$, 0.8 mol of NaOH, and 0.02 mol of Na_2CO_3 were slowly mixed under vigorous stirring, maintaining the pH between 8 and 10, at 343 ± 5 K. The mixture was heated at this temperature for 15 h under stirring. The precipitate was washed several times until the solution was free of chloride ions ($AgNO_3$ test). The products were dried at 313 K. They contain both Cl^- and CO_3^{2-} as charge-compensating anions, as established from the chemical analysis data reported in Table 1. These samples will be referred to as HT(3)–Cl–CO_3.

Using the same procedure, another sample was prepared by mixing 0.25 mol $MgCl_2 \cdot 6H_2O$, 0.1 mol $AlCl_3 \cdot 6H_2O$, 0.8 mol NaOH, and 0.02 mol Na_2CO_3. It is referred to below as HT(2.5)–Cl–CO_3.

Procedure of Anion Exchange

The exchange of Cl^- anions was performed by contacting the hydrotalcite with a solution of Na_2CO_3; 2 g of HT(3)–Cl–CO_3 and HT(2.5)–Cl–CO_3 were dispersed in a 1.5×10^{-3} *M* solution of sodium carbonate and stirred at 343 K for 2 h. After filtration, the solids were washed and dried at 313 K. These samples will be referred to as HT(3)–CO_3-A and HT(2.5)–CO_3-A. In order to achieve a higher degree of exchange, a second exchange was carried out on HT(3)–CO_3-A. This sample will be referred to below as HT(3)–CO_3-B.

TABLE 1

Compositions of the Samples and *c* Parameters

Sample	Composition	*c* (Å)
HT(3)–Cl–CO_3	$Mg_{0.74}Al_{0.26}(OH)_{2.11}(CO_3^{2-})_{0.08}Cl_{0.15} \cdot 0.32H_2O$	23.63
HT(3)–CO_3-B	$Mg_{0.74}Al_{0.26}(OH)_{2.15}(CO_3^{2-})_{0.17} \cdot 0.59H_2O$	23.37
HT(2.5)–Cl–CO_3	$Mg_{0.71}Al_{0.29}(OH)_{1.86}(CO_3^{2-})_{0.10}Cl_{0.14} \cdot 0.61H_2O$	23.22
HT(2.5)–CO_3-B	$Mg_{0.71}Al_{0.29}(OH)_{2.03}(CO_3^{2-})_{0.19}Cl_{0.06} \cdot 0.60H_2O$	23.06

Characterization

X-ray powder diffraction patterns were recorded with a CGR Theta 60 instrument using Cu $K\alpha_1$ radiation.

DTA and TGA analyses were carried out in a Setaram microbalance, operated under a flow of dry nitrogen at a heating rate of 5 K/min.

Infrared spectra of self-supported wafers were recorded with a Perkin–Elmer 1760 X FT-IR instrument equipped with a MCT detector. The quartz cell with KBr windows was connected to a vacuum line (10^{-3}–10^{-6} Torr) for thermal treatments in a controlled atmosphere.

Before characterization, the samples were first calcined to decompose the carbonates and possible carbon deposits. The calcinations were carried out in a thin bed configuration using a horizontal furnace flushed with an air flow of about 100 ml min^{-1}. The heating rate was 50 K h^{-1}, and the final temperature was maintained for 5 h.

Microcalorimetric Measurements

The adsorption of CO_2 was followed both by calorimetry and measurements of uptake using the experimental apparatus described elsewhere (24). After outgassing the sample at 673 K, CO_2 was introduced in small increments. The heat of adsorption of CO_2 can be taken as a measure of the basic strength of the adsorption sites, and therefore the distribution in strengths of basic sites was obtained using the differential heat of adsorption as a function of coverage.

Catalysis

The kinetics of the condensation reaction were followed in a stirred stainless-steel reactor, under an atmosphere of nitrogen at 383 K and 2.5 bar; 0.8 g of catalyst in ethanol was employed.

Benzaldehyde was a Merck product. Benzaldehyde/acetone molar ratios were between 2 and 7×10^{-2}. Typically, 0.6 mol of acetone was added to 0.04 mol of benzaldehyde; the volume was completed to 80 ml with ethanol and 0.8 g of catalyst was added.

The reaction products were analyzed with a Delsi 30 chromatograph equipped with an OV1 (25 m long) capillary column.

RESULTS

Representative X-ray diffraction patterns of HT(2.5)–Cl–CO_3 and HT(2.5)–CO_3-B are shown in Fig. 1. They are characteristic of well crystallized products with a bidimensional structure. The *c* parameter has been calcu-

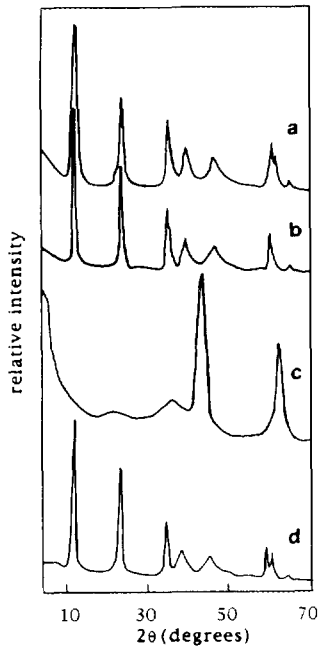

FIG. 1. XRD profile of (a) HT(2.5)–Cl–CO_3, (b) HT(2.5)–CO_3-B, (c) HT(2.5)–CO_3-B calcined at 723 K, and (d) HT(2.5)–CO_3-B calcined at 723 K and rehydrated.

lated from the (003) reflection at around 10° 2θ. It decreases slightly when replacing Cl^- by CO_3^{2-} and with increasing layer charge (Table 1).

The structural formulas given in Table 1 were established from the chemical analyses of the solids and the thermogravimetric data reported in Fig. 2. As suggested by other authors (8), the amount of structural water was obtained by subtracting the amount of physically adsorbed water lost at 378 K from the initial weight loss on the TGA diagram. The Mg/Al ratio of the solid phase is nearly equal to that in the synthesis solution, which was chosen in the optimal range for obtaining the double-hydroxide structure.

In all the samples, an excess of anionic charge is observed. In spite of the high selectivity of these layered double hydroxides for carbonate ions, chemical analysis reveals a significant amount of Cl^- which represents 50% of the anionic charge of the initial samples. A similar observation was reported for the precipitation at low supersaturation in the case of nitrate ions (4). The chemical composition of HT(3)–CO_3-B shows the total removal of Cl^- after two exchanges of the initial sample.

Thermal Treatment

Upon calcination of HT(2.5)–CO_3-B at 723 K, the XRD pattern shows the transformation of the hydrotalcite into a mixed oxide with MgO structure (Fig. 1c). Above 1073 K, the spectrum of $MgAl_2O_4$ with a spinel structure is obtained (not shown here).

The thermograms reported in Fig. 2 show a two-step weight loss. The first step, below 473 K, is attributed to loosely bound water in the interlayer space, and the second one, at 610–645 K to the simultaneous dehydroxylation and decarbonation of the lattice. The thermograms of HT(3)–CO_3-B (Fig. 2a) and HT(2.5)–CO_3-B (Fig. 2c) show that the exchange of Cl^- anions for CO_3^{2-} has only a small influence on the total weight loss, but the second peak is shifted by 15 K toward higher temperatures for HT(3)–CO_3-B and by 35 K for HT(2.5)–CO_3-B and a shoulder appears at 575 K. The chlorine replacement induces the formation of several types of carbonate species and, particularly, of strongly bonded ones.

The IR spectra of HT(2.5)–Cl–CO_3 and HT(2.5)–CO_3-B outgassed at increasing temperatures up to 1073 K are shown in Figs. 3 and 4, respectively. After outgassing at

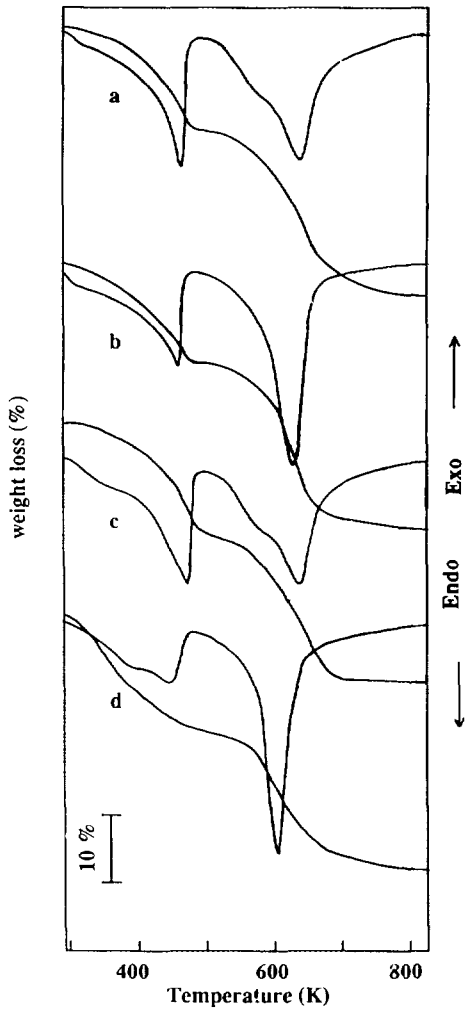

FIG. 2. DTA–TGA curves of (a) HT(3)–CO_3-B, (b) HT(3)–Cl–CO_3, (c) HT(2.5)–CO_3-B, and (d) HT(2.5)–Cl–CO_3.

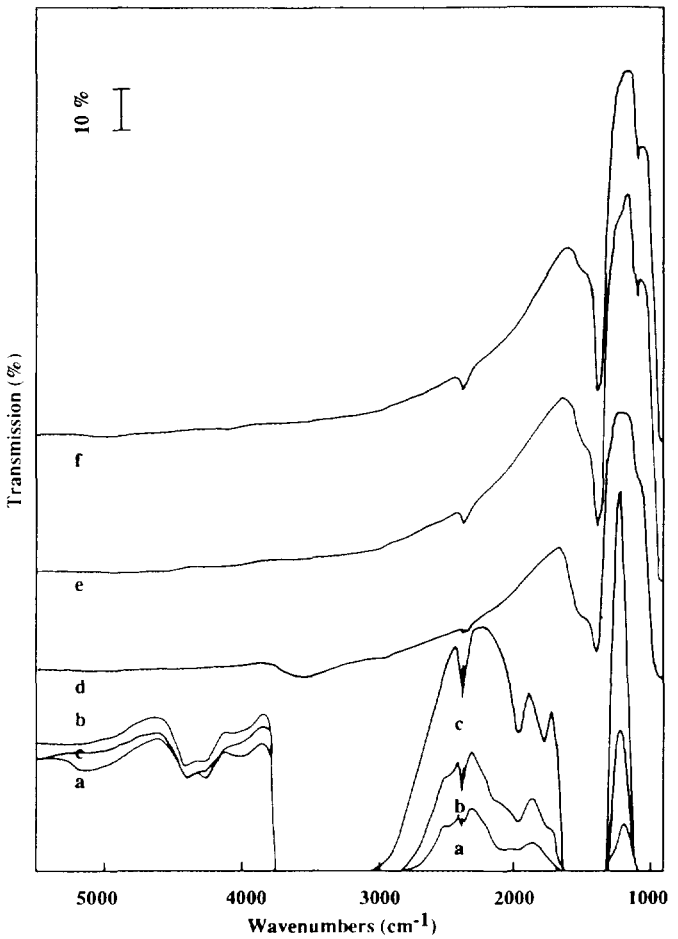

FIG. 3. IR spectra of HT(2.5)–Cl–CO_3 outgassed at (a) room temperature, (b) 373 K, (c) 473 K, (d) 723 K, (e) 923 K, and (f) 1073 K.

room temperature (spectrum a), no transmittance is observed in the ranges 2700–3800 cm^{-1} (related to water and hydroxyl groups), 1300–1650 cm^{-1} (CO_3^{2-} and water), and 900–1000 cm^{-1} (carbonates and Mg–O–Mg or Al–O–Mg bonds). This is due to the high hydroxyl and carbonate content of the samples.

Information may be drawn from the weak bands observed at 5075, 4383, 4244, and 3990 cm^{-1} up to 673 K, and in the 2100–1700 cm^{-1} range, which are due to combination or overtone modes. In particular, the 5075-cm^{-1} band is due to a carbonate species. Their positions are not constant. They are characteristics of the multiplicity of the carbonate species.

Heating at temperatures higher than 473 K improves the transparency of the opaque regions, due to the simultaneous loss of water and carbon dioxide. The carbonate bands become weaker and a new band appears at 1079 cm^{-1}, decreasing in intensity with temperature, attributed to the symmetrical stretching of the O–C–O bonds. This variation is accounted for by a progressive increase in the symmetry of the carbonate species with the removal of the interlayer water.

The treatment temperature at which total transparency occurs in the 1300–1680 cm^{-1} range depends on the carbonate content of the samples. Defined bands of carbonates are clearly observed at 1079, 1390, and 1507 cm^{-1} after outgassing HT(2.5)–Cl–CO_3 at 723 K (Fig. 3d) or at 1073 K for HT(2.5)–CO_3-B (Fig. 4f), with bands at 1079, 1383, and 1518 cm^{-1}. These results are in line with the shift toward higher temperatures of the thermogravimetric peaks after total exchange of the chloride ions. When these ions are initially present, as in the representative HT(2.5)–Cl–CO_3 sample, they are not vaporized as HCl upon calcination, and their field induces asymmetric carbonate species with different thermal stabilities and which are decomposed at a lower temperature. Carbonates persisting at temperatures higher than 1073 K are probably occluded in the structure.

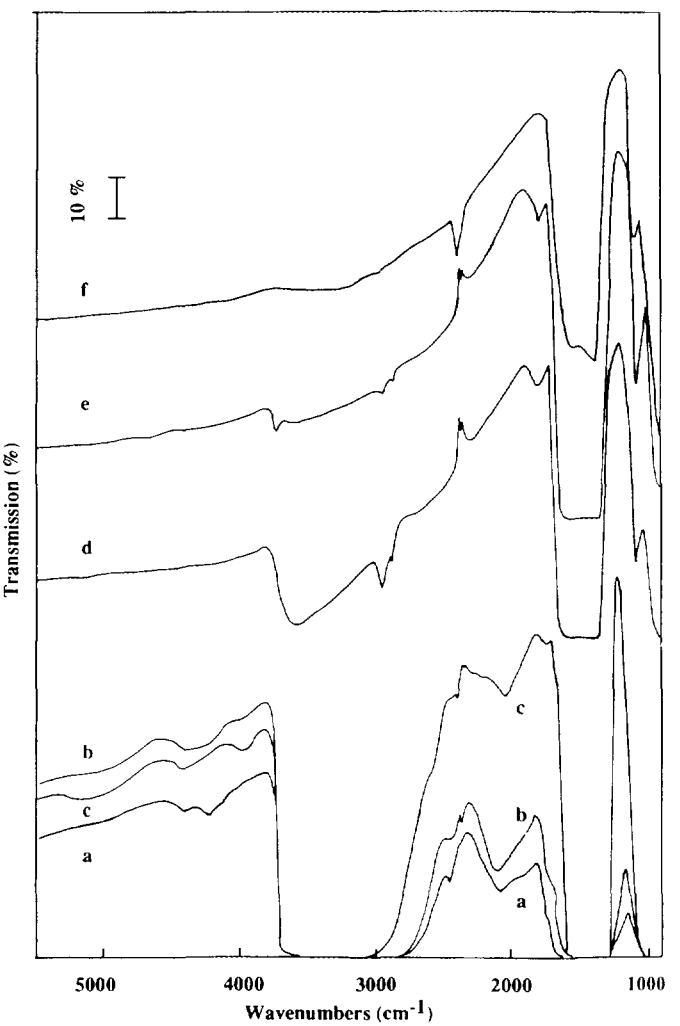

FIG. 4. IR spectra of HT(2.5)–CO_3-B outgassed at (a) room temperature, (b) 373 K, (c) 573 K, (d) 673 K, (e) 823 K, and (f) 1073 K.

Except after the early stage of the thermal treatment, when physisorbed water is eliminated, the evolution of gases does not give rise to any new band, even though the carbonate species is usually rather sensitive to the environment. This indicates that there are no rearrangements in the coordinative situation of the carbonate species.

In the hydroxyl region, the bands observed at around 3600 and 3740 cm^{-1} after outgassing HT(2.5)–Cl–CO_3 at 723 K (Fig. 3d) and HT(2.5)–CO_3-B at 673 K (Fig. 4d) are due, respectively, to hydrogen-bonded and free OH groups, as generally reported for the parent MgO (25).

In both samples, complete dehydroxylation is achieved upon calcination at 823 K, a temperature higher than that in the DTA analyses, due to the smaller heating rate during outgassing.

Carbonation of the Mixed Oxides

Calcined HT(2.5)–Cl–CO_3 samples were contacted with CO_2 with the aim to study the adsorption capacities and the reversibility of the carbonation process of the mixed oxides. Information on the nature of the active sites might also be expected due to the interaction of CO_2 with basic and acid sites.

The adsorption isotherms at 423 K of HT(2.5)–Cl–CO_3 and HT(2.5)–CO_3-B, previously outgassed at 673 K for 15 h, reveal the higher adsorption capacity of the fully carbonated sample (Fig. 5). The amount of CO_2 adsorbed increases with the calcination temperature as shown, for example, by the adsorption isotherms at 300 K for HT(2.5)–Cl–CO_3 calcined up to 850 K (Fig. 5).

The quasi-differential heats of adsorption of CO_2 on the samples as a function of the amount adsorbed are shown in Fig. 6. The results obtained for MgO, a well known basic compound with high surface area (200 $m^2 g^{-1}$), outgassed at 673 K, are also given. The heat of adsorption increases with calcination temperature for HT(2.5)–Cl–CO_3. Only a few sites have heats of adsorption higher than those of MgO.

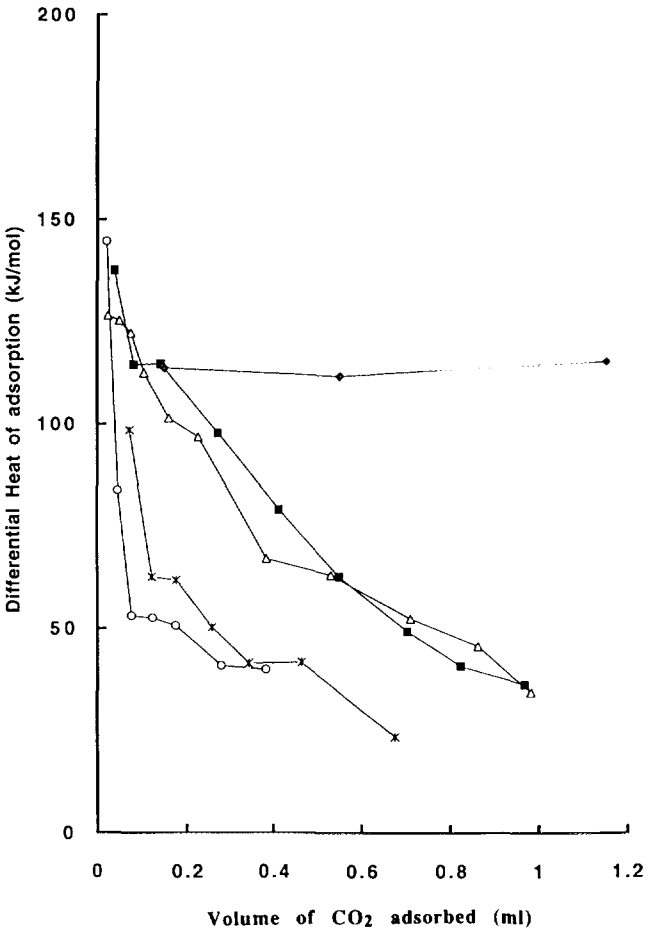

FIG. 6. Variation of the differential heat of CO_2 adsorption vs CO_2 adsorbed for HT(2.5)–Cl–CO_3 noncalcined (○) and calcined at (*) 673 K, (△) 800 K, and (■) 850 K, and for (◆) MgO.

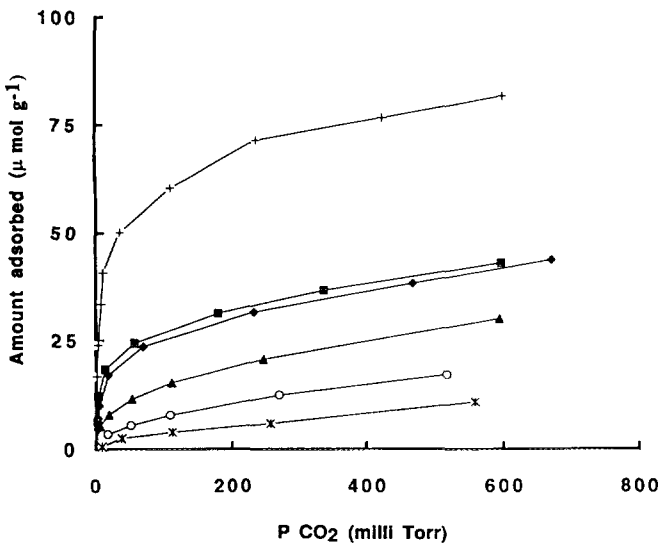

FIG. 5. CO_2 adsorption isotherms at 423 K for (*) HT(2.5)–Cl–CO_3, (+) HT(2.5)–CO_3-B, and at 300 K for HT(2.5)–Cl–CO_3 (○) uncalcined and calcined at (▲) 673 K, (◆) 800 K, and (■) 850 K.

The IR spectrum of HT(2.5)–Cl–CO_3 outgassed at 723 K (Fig. 7a) shows the same bands in the hydroxyl and carbonate domains as those previously observed (Fig. 3d). Upon addition of 20 Torr of CO_2 at room temperature, the carbonate bands at 1385 and 1488 cm^{-1} remain unchanged and a new band appears at 1685 cm^{-1} which may be assigned to a bicarbonate species (26) (Fig. 7b).

Note that the intensity of the bicarbonate band is rather weak, thus showing that the extent of reaction with basic hydroxyls is limited. Apparently, there is no reaction with basic O^{2-} centres, whereas there is extensive interaction with Lewis acid sites. Indeed, two intense bands appear at 2349 and 2367 cm^{-1}, which are assigned to CO_2

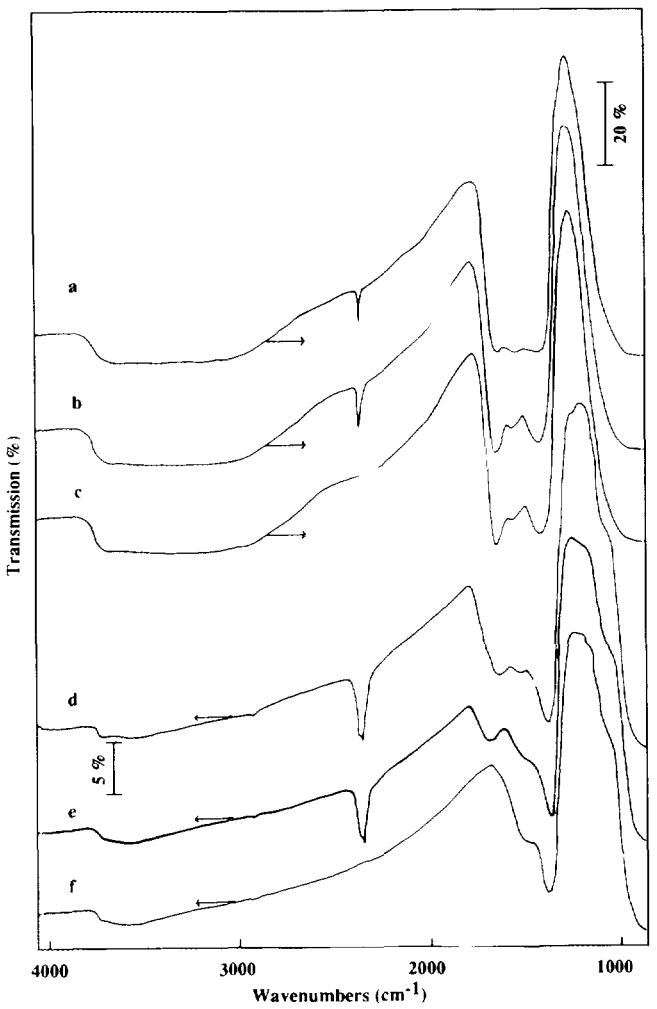

FIG. 7. IR spectra of HT(2.5)–Cl–CO_3 (a) outgassed at 723 K, (b) after adsorption of CO_2 at 20 Torr, (c) after 3 days equilibrium, (d) after addition of H_2O, (e) after addition of CO_2 at 25 Torr, and (f) after outgassing at 373 K.

linearly coordinated to Lewis acid sites, such as Mg^{2+} and Al^{3+} cations (Fig. 7b).

After equilibration for 3 days in the cell, the only modification observed in the spectrum of HT(2.5)–Cl–CO_3 is an increase of the bicarbonate band (Fig. 7c). The spectrum obtained is different from that of the hydrotalcite sample outgassed at room temperature (Fig. 3a) and shows that the carbonation process is essentially superficial, the internal sites being inaccessible to CO_2. When 4.5 Torr of H_2O were introduced at 373 K on the mixed oxide previously calcined at 723 K and treated with CO_2, the spectrum of the original hydrotalcite was restored (Fig. 7f).

Note that one linear CO_2 species at 2343 cm^{-1} survives the carbonation and water treatments. Thus, at moderate calcination temperature, the transformation of the hydrotalcite into a mixed oxide is partly reversible. This is also confirmed by X-ray diffraction. Indeed the (003), (006), and (009) peaks characteristic of the lamellar structure were restored when the mixed oxide, resulting from a hydrotalcite sample calcined below 873 K, was dispersed in carbonated water or contacted with wet air for several days (Fig. 1d). This memory effect of the hydrotalcite has been previously reported by other authors (4, 13).

Catalytic Tests

Preliminary experiments were performed using different stirring speeds and catalyst particle sizes to avoid diffusion limitations. Between 600 and 1000 rpm and for particle sizes <0.5 mm, the reaction rate is not limited by diffusion processes.

The Claisen-Schmidt homogeneous (27–32) and heterogeneous (33, 34) condensation of benzaldehyde with various ketones is a relatively well explored reaction. The condensation of benzaldehyde with excess acetone gives principally benzalacetone (4-phenyl-3-butene-2-one):

$$C_6H_5CHO + CH_3COCH_3 \rightarrow C_6H_5{-}CHOH{-}CH_2{-}COCH_3$$

$$C_6H_5CH{=}CH{-}\overset{\overset{O}{\|}}{C}{-}CH_3$$

Excess acetone reduces the formation of dibenzalacetone formed by further reaction of benzaldehyde with benzalacetone.

The kinetics of the transformation of benzaldehyde (excess acetone: 15 equivalents) appears to be pseudo-first-order in benzaldehyde. According to the classical mechanism in solution, the first step of the condensation reaction between benzaldehyde and acetone using hydrotalcite as a catalyst would be the proton abstraction from acetone by the basic sites of the solid.

When the reaction was performed with substituted benzaldehydes, the experimental rate constant increased as a function of the nucleophilic strength of the substituents (p-NO_2 > m-Cl > p-Cl > Me > p-OMe). A linear relationship was obtained when plotting the logarithm of the experimental pseudo-first-order rate constants against the corresponding Hammett substituent coefficients. A good correlation (correlation coefficient = 0.97) was obtained using the σ^+ values (35) with a reaction constant ρ of 0.7 (Fig. 8).

The positive value of the reaction constant, ρ, is indicative of a reaction facilitated by a low electron density at the reaction centre. The sign and the value of ρ are of the same magnitude as those found in homogeneous catalysis with NaOH (36) or in heterogeneous catalysis with Al_2O_3 (33). Moreover, the homogeneous acid catalysed aldoli-

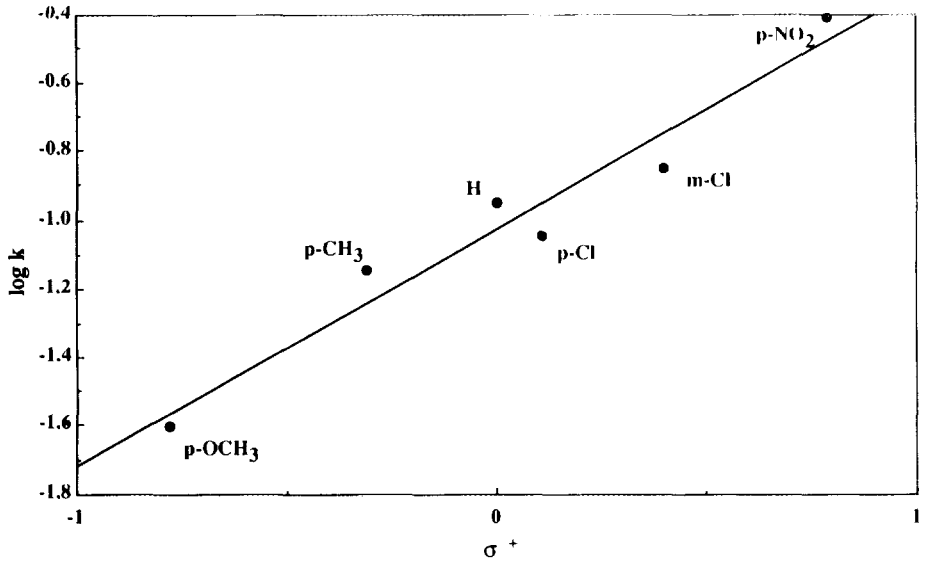

FIG. 8. Hammett correlation for the condensation reaction of substituted benzaldehydes and acetone over HT(2.5)–Cl–CO_3.

zation and aldol dehydration are characterized by a negative value of the ρ constant.

These results (peudo-first-order in benzaldehyde with a positive value of the Hammett reaction constant) support the assumption that the rate-determining step is the nucleophilic addition of the carbanion to C=O of benzaldehyde to yield the corresponding aldol (4-hydroxy-4-phenyl butane-2-one).

These results, which exhibit a strong analogy with the homogeneous base-catalyzed condensation reaction, allow us to conclude that the condensation of benzaldehyde and acetone is catalyzed by the basic sites of the catalyst.

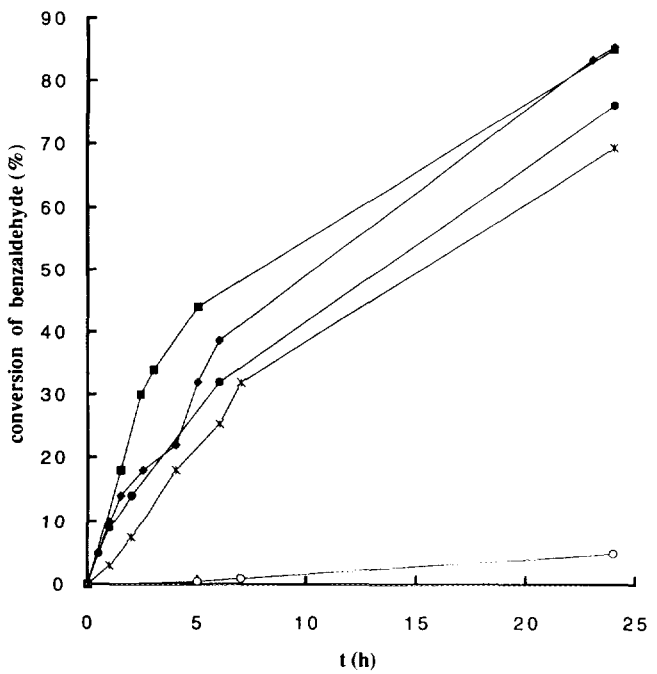

FIG. 9. Influence of the carbonate content of the hydrotalcite in the conversion of benzaldehyde and comparison with pyridine and piperidine: (■) piperidine, (◆) HT(3)–CO_3-B, (●) HT(3)–CO_3-A, (*) HT(3)–Cl–CO_3, and (○) pyridine.

The influence of the carbonate content of the hydrotalcite on the catalytic activity has been studied over HT(3)–Cl–CO_3, HT(3)–CO_3-A, and HT(3)–CO_3-B activated at 723 K. The conversion vs time curves are shown in Fig. 9. All the curves tend toward a plateau beyond 20 h of reaction. The most remarkable feature is that the level of activity increases with the carbonate content of the sample.

The exchange of the last percentages of the remaining chlorides has a marked effect on the catalytic activity. This may be related to the presence of sites with differential heat of adsorption of CO_2 as high as 150 kJ/mol, as seen previously for HT(2.5)–Cl–CO_3.

In order to determine the influence of the calcination temperature, HT(3)–Cl–CO_3 was activated at different temperatures between 723 and 1023 K. The initial reaction rates determined after calcination at different temperatures are reported in Table 2. A maximum is observed at 823 K and a low level of activity is observed for activation temperatures of 923 K and higher.

The X-ray diffraction spectra of the active catalysts after reaction show, in all cases, the characteristic pattern of the hydrotalcite structure.

The activity may also be related to structural parameters of the hydrotalcite. The respective influence of Mg/Al ratio and anion exchange is illustrated in Fig. 10. The

TABLE 2

Initial Reaction Rates in the Condensation Reaction of Benzaldehyde and Acetone with HT(3)–CO_3-B Calcined at Different Temperatures

Calcination temperature (K)	Initial rate (mol liter $^{-1}$ h $^{-1}$)
723	0.027
823	0.034
923	0.012
1023	0.012

initial reaction rates are reported for the two series of hydrotalcites with Mg/Al of 2.5 and 3, respectively, as a function of their C_3^{2-} content. The samples were all activated at 723 K. As reported previously, the activity increases with the CO_3^{2-} content of the sample, but it is also noticeable that for a similar CO_3^{2-} content, it increases with the Mg/Al ratio of the mixed hydroxide.

In order to compare the catalytic activity of the hydrotalcites with those of organic bases currently used in homogeneous catalysis, the test reaction was also carried out in the presence of pyridine (pK_a = 8.8) and piperidine (pK_a = 11.12) in place of the hydrotalcites. The amounts of base added were evaluated on the basis of the number of aluminium atoms in the sample.

The results reported in Fig. 9 show that, whatever their degree of exchange, the hydrotalcites are more basic than pyridine, and a basicity similar to that of piperidine is found for the fully exchanged HT(3)–CO_3-B having sites with pK_a higher than 11.

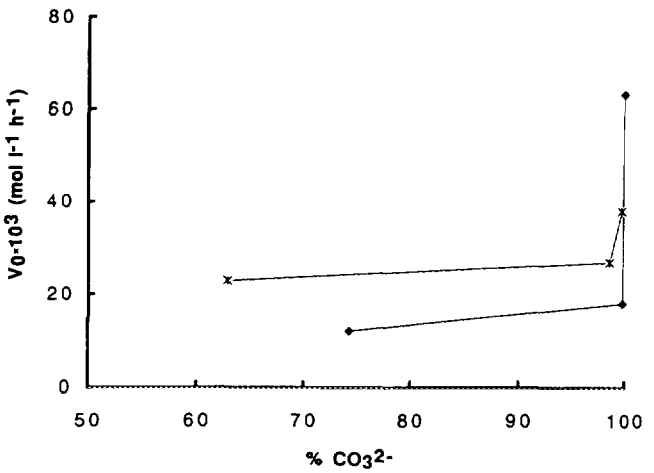

FIG. 10. Variation of the initial reaction rate of benzaldehyde with acetone vs CO_3^{2-} content for hydrotalcites with Mg/Al ratios of (◆) 2.5 and (*) 3.

DISCUSSION

It is possible to modify the basicity of hydrotalcites by a judicious control of the carbonate content, the activation temperature and the Mg/Al ratio of the layers. The first parameter could be adjusted by anion exchange and the latter one at the preparation step. Upon calcination, the hydrotalcite is transformed with simultaneous elimination of CO_2 and water. This is achieved without phase segregation up to 673 K. Above this temperature, a Mg(Al)O mixed oxide appears. CO_2 and water are released without modification of the nature of the neighbor carbonate entitites. This is in agreement with the results of Reichle *et al.* (14), which show that upon heating Mg–Al hydrotalcites, water and CO_2 are released by a cratering mechanism rather than by exfoliation, and that the crystal morphology is preserved. A spinel-like phase, $MgAl_2O_4$, is observed at 1073 K with persistence of some carbonate species occluded in the structure. The most active catalysts obtained upon calcination of hydrotalcite are those which contain the mixed oxide phase.

Due to the memory effect, the hydrotalcite could be partly restored upon carbonation of the calcined sample in wet atmosphere. This effect is currently observed after catalytic reactions which, as in aldol condensation, produce water.

The catalytic activity regularly increases with the decomposition of the least stable carbonates, and goes through a maximum at a calcination temperature of 773 K, where the more stable carbonates species are not totally eliminated as shown by the TG and IR analysis data. These thermally stable carbonates are rather comparable to those found by King and Garces (37) in K–X, Rb–X, and Cs–X zeolites calcined at 720 K and may thus be similarly attributed to the high basic strength of these species. Dehydroxylation, which begins well before the formation of the spinel phase, results in a decrease of activity. This suggests that the basic sites are essentially the hydroxyl groups rather than O^{2-} species. Indeed the IR spectra clearly show that some hydroxyl groups are still present after outgassing at 720 K, and that upon CO_2 adsorption, bicarbonates rather than CO_3^{2-} species were preferentially formed.

Under the reaction conditions employed in this work, the catalyst is always in contact with the water produced by the reaction and, consequently, the catalytic active sites are the OHs of moderate strength. Considering the aldolisation activities, the basic strength of the most active hydrotalcites is comparable to that of piperidine in homogeneous medium, thus indicating that basic sites with pK values of at least 11 are present, as previously reported by Corma *et al.* (21).

However, the small number of strong basic sites adsorbing CO_2 with 140 kJ/mol probably originate from O^{2-}

species. Indeed, they are observed only after activation at high temperature, resulting from the evolution of CO_2 from the more stable CO_3^{2-} species, or from the removal of Cl^- adsorbed on the least acidic sites, due to the electrophilic nature of these two anionic species. This also has a practical consequence. The calcined hydrotalcites stored in air partly lose their activity due to the carbonation process with CO_2 from the ambient atmosphere and therefore must be reactivated before use.

The enhancement in activity after exchange of the last chloride ions is similar to that observed in acidic zeolites, where the exchange of the last Na^+ cations with H^+ liberates acid sites of high strength and increases the catalytic activity.

Lewis acid sites are also present in hydrotalcites; they are due to Al^{3+} and Mg^{2+} cations. Aldol condensation could be performed by acidic and basic centers as in the vapor-phase reaction of methyl propionate and formaldehyde with alkali-exchanged X and Y zeolites (38). In the present case, the acidic sites are not strong enough to operate the aldol condensation, but they are responsible for the dehydrating activity of hydrotalcites This also confirms the influence of the preparation conditions on the surface properties of hydrotalcites as reported by McKenzie *et al.* (39). These authors did not detect a significant acidity on hydrotalcite, as compared to a MgO/Al_2O_3 mixture with similar composition.

The increase of the initial reaction rates (see Table 3) with Mg/Al ratio of the hydrotalcites must be related to an increase of the amount of the OH basic sites of moderate strength rather than to the formation of new sites of higher strength, following a mechanism similar to those observed in zeolites. Indeed, it is widely accepted that in zeolites, when the Si/Al ratio increases, the interaction between neighboring sites is reduced, creating acid sites of high strength. The different behavior observed in the case of hydrotalcites has also been reported by Corma *et al.* (21). Increasing the Mg/Al ratio of the hydrotalcites from 2.33 to 3 resulted in an increase of the total amount of basic sites, but the proportion of those catalyzing the condensation of benzaldehyde and ethyl bromoacetate (corresponding to $pK_a = 16.5$) decreased.

TABLE 3

Initial Reaction Rates in the Condensation Reaction of Benzaldehyde and Acetone vs the Carbonate Content of the Hydrotalcites

Mg/Al	CO_3^{2-} (% of charge)	$v_0 \times 10^3$ (mol liter^{-1} h^{-1})
2.5	74.30	12
	99.85	18
	99.93	63
3	62.80	23
	98.54	27
	99.69	38

REFERENCES

1. Reichle, W. T., *Chemtech.* **1,** 58 (1986).
2. Jones, W., and Chibwe, M., *in* "Pillared Layered Structures—Current Trends and Applications" (I. V. Mitchell, Ed.), p. 67. Elsevier Applied Science, London and New York, 1990.
3. De Roy, A., Forano, C., El Malki, K., and Besse, J. P., *in* "Synthesis of Microporous Materials" (M. L. Occelli and H. Robson, Eds.), Vol. 2, p. 108. Van Nostrand–Reinhold, New York, 1992.
4. Cavani, F., Trifirò, F., and Vaccari, A., *Catal. Today* **2,** 11 (1991).
5. Corrado, K. A., Kostapapas, A., and Suib, S. L., *Solid State Ionics* **26,** 77 (1988).
6. Miyata, S., Kumura, T., and Shimada, M., U.S. Patent, 3.879.523 (1975).
7. Serna, C. J., Rendon, J. L., and Iglesias, J. E., *Clays Clay Miner.* **30,** 180 (1982).
8. Miyata, S., *Clays Clay Miner.* **23,** 369 (1975).
9. Bish, D. L., *Bull. Miner.* **103,** 170 (1980).
10. Miyata, S., and Hirose, T., *Clays Clay Miner.* **26,** 441 (1978).
11. Woltermann, G. M., U.S. Patent 4.454.244 (1984).
12. Drezdzon, M. A., *Inorg. Chem.* **27,** 4628 (1988).
13. Rey, F., and Fornés, V., *J. Chem. Soc. Faraday Trans.* **88,** 2233 (1992).
14. Reichle, W. T., Kang, S. Y., and Everhardt, D. S., *J. Catal.* **101,** 352 (1986).
15. Rouxhet, P. G., and Taylor, H. F. W., *Chimia* **23,** 480 (1969).
16. Brindley, G. W., and Kikkawa, S., *Clays Clay Miner.* **28,** 87 (1980).
17. Suzuki, E., and Ono, Y., *Bull. Chem. Soc. Jpn.* **61,** 1008 (1988).
18. Reichle, W. T., *J. Catal.* **94,** 547 (1985).
19. Rameswaran, M., Rightor, E. G., Dimotakis, E. D., and Pinnavaia, T. J., *in* "Proceedings, 9th International Congress on Catalysis, Calgary, 1988" (M. J. Phillips and M. Ternan, Eds.), Vol. 2, p. 783. Chem. Inst. Canada, Ottawa, 1988.
20. Suzuki, E., Okamoto, M., and Ono, Y., *J. Mol. Catal.* **61,** 283 (1990).
21. Corma, A., Fornés, V., Martin-Aranda, R. M., and Rey, F., *J. Catal.* **134,** 58 (1992).
22. Corma, A., and Martin-Aranda, R., *J. Catal.* **130,** 130 (1991).
23. March, J., "Advanced Organic Chemistry," third ed. Wiley, New York, 1985.
24. Auroux, A., *in* "Les Techniques Physiques d'Etude des Catalyseurs" (B. Imelik and J. C. Védrine, Eds.), p. 823. Editions Technip, Paris, 1988.
25. Coluccia, S., Lavagnino, S., and Marchese, L., *J. Chem. Soc. Faraday Trans.* 1 **83,** 477 (1987).
26. Busca, G., and Lorenzelli, V., *Mater. Chem.* **7,** 89 (1982).
27. Nitikin, J. K., *Zh. Obshch. Khim.* **7,** 2264 (1937).
28. Gettler, J. D., and Hammett, L. P., *J. Am. Chem. Soc.* **65,** 1824 (1943).
29. Kandlikar, S., Sethuram, B., and Rao, T. N., *J. Prakt. Chem.* **321,** 131 (1979).
30. Kandlikar, S., Sethuram, B., and Rao, T. N., *Z. Phys. Chem.* **95,** 87 (1975).
31. Noyce, D. S., and Snyder, L. R., *J. Am. Chem. Soc.* **81,** 620 (1959).
32. Noyce, D. S., and Reed, W. L., *J. Am. Chem. Soc.* **81,** 624 (1959).

33. Nondek, L., and Malek, J., *Collect. Czech. Chem. Commun.* **45,** 1812 (1980).
34. Aguilera, A., Alcantara, A. R., Marinas, J. M., and Sinisterra, J. V., *Can. J. Chem.* **65,** 1165 (1987).
35. Ritchie, C. D., and Sager, F., *Prog. Phys. Org. Chem.* **2,** 323 (1964).
36. Coombs, E., and Evans, D. P., *J. Chem. Soc.,* 1295 (1940).
37. King, S. T., and Garces J. M., *J. Catal.* **104,** 59 (1987).
38. Wierzchowski, P. T., and Zatorski, L. W., *Catal. Lett.* **9,** 411 (1991).
39. McKenzie, A. L., Fishel, C. T., and Davis, R. J., *J. Catal.* **138,** 547 (1992).